Available online at www.sciencedirect.com
ScienceDirect
C. R. Geoscience 341 (2009) 394–405
COMPTES RENDUS GEOSCIENCE

Geodynamics

Melt initiation and mantle exhumation at the Iberian rifted margin: Comparison of pure–shear and upwelling-divergent flow models of continental breakup

Rosie Fletcher [a], Nick Kusznir [b,*], Mike Cheadle [c]

[a] *Statoil (UK) Ltd., Statoil House, 11a Regent Street, London, SW1Y 4ST, UK*
[b] *Department of Earth and Ocean Science, University of Liverpool, Liverpool, L69 3GP, UK*
[c] *Department of Geology and Geophysics, University of Wyoming, Laramie, Wyoming, USA*

Received 31 January 2008; accepted after revision 15 December 2008
Available online 28 February 2009

Written on invitation of the Editorial Board

Abstract

Observations of a wide (up to 170 km) zone of exhumed continental mantle on the Iberian non-volcanic rifted margin have questioned our understanding of the processes involved in continental breakup and seafloor spreading initiation. Models of continental lithosphere thinning by pure–shear predict melt generation before continental breakup, and thus do not predict the exhumation of mantle. Whilst the paucity of volcanism during breakup on the Iberian margin may be explained by invoking a cooler or depleted mantle, or by poor melt extraction, other lithosphere scale processes may play an important role during continental breakup. We compare melt production predicted by pure–shear models of continental lithosphere thinning to that predicted by an upwelling–divergent flow model, using kinematic constraints appropriate to the Iberian margin. The upwelling–divergent flow model predicts exhumation of a more than 50 km-wide zone of continental mantle prior to melt initiation, and we suggest that this mode of lithosphere deformation may play an important role in the formation of rifted margins. ***To cite this article: R. Fletcher et al., C. R. Geoscience 341 (2009).***

Résumé

Initiation de la fusion et exhumation du manteau à la marge de rift ibérique : comparaison entre cisaillement pur et modèles d'« *upwelling* – flux divergent » de fracture continentale. Des observations sur une vaste zone (supérieure à 170 km) du manteau continental exhumé sur la marge ibérique de rift, non volcanique, questionnent à propos de la compréhension des processus impliqués dans l'initiation de la fracturation continentale et de l'expansion du plancher océanique. Des modèles d'amincissement de la lithosphère continentale par cisaillement pur prédisent une génération de fusion avant la fracturation continentale et, de ce fait, ne prédisent pas l'exhumation du manteau. Tandis que l'absence de volcanisme pendant la fracturation continentale sur la marge ibérique peut s'expliquer en invoquant un manteau appauvri et plus frais, ou une faible extraction de produits de fusion, d'autres processus à l'échelle de la lithosphère peuvent jouer un rôle important lors de la fracturation continentale. Nous comparons la production de matériau de fusion prédite par des modèles de cisaillement pour de l'amincissement de la lithosphère continentale à celle produite par un modèle « *upwelling*– flux divergent », utilisant des contraintes cinématiques appropriées à la marge ibérique, le modèle « *upwelling* -flux divergent » prédit l'exhumation d'une zone de plus de 50 km de large de manteau continental avant

* Corresponding author.
E-mail address: n.kusznir@liv.ac.uk (N. Kusznir).

1631-0713/$ – see front matter
doi:10.1016/j.crte.2008.12.008

l'initiation de la fusion et nous proposons que ce mode de formation de la lithosphère joue un rôle important dans la formation des marges. ***Pour citer cet article : R. Fletcher et al., C. R. Geoscience 341 (2009).***

Keywords: Continental margins; Rifting; Continental breakup; Melting; Exhumed mantle; Lithosphere thinning

Mots clés : Marges continentales ; *Rifting* ; Fracture continentale ; Fusion ; Manteau exhumé ; Amincissement continental

1. Introduction

A wide transitional zone of exhumed serpentinised continental mantle, isolated continental fault blocks and thin oceanic crust is observed between unequivocal continental and oceanic crust at some non-volcanic rifted continental margins. Such transition zones are termed zones of exhumed continental mantle (ZECM) and have been documented at the Iberian–Newfoundland and Greenland–Labrador conjugate margins and the remnants of the margins of the Liguria-Piemonte ocean now exposed in the Alps [3,4,9,33,23,44]. The exhumation of mantle implies that thinning and rupture of continental crust occurred in the absence of significant volcanic addition, which is difficult to explain if continental breakup occurs by pure–shear stretching and thinning. The Iberian margin is well studied in terms of structure and kinematics, and we use it in this paper as a type-locality to test models of continental breakup which include melt generation by decompression melting.

Pure–shear thinning of continental lithosphere, first quantified by [24], is widely thought to be the process responsible for intracontinental basin formation. The pure–shear model predicts that the magnitude of stretching and thinning, accommodated by both brittle faulting and ductile processes, is uniform with depth. The pure–shear model has also been used to explain continental breakup and rifted margin formation [5,26], although it predicts far more melt than is observed or is suggested by the seismic velocity structure at the Iberian margin [26,35]. The lack of volcanism may be explained by an anomalously cool mantle prior to breakup [26,35,30], a depleted mantle source [30] or initially slow extension or distributed thinning [42,15]. However, observations of depth-dependent lithospheric stretching, exhumation of lower continental crust and continental mantle, and apparently anomalous volcanism at non–volcanic and volcanic rifted margins, including conjugate pairs [36,8,11,20], suggest that lithosphere-scale deformation processes other than pure–shear may play an important role during continental breakup. Upwelling–divergent flow (UDF), a mode of deformation similar to that envisaged for mid ocean ridges [6,34], is a possible lithospheric thinning mechanism which may operate as continental breakup evolves into seafloor spreading [21,19]. The UDF model implies that thermal buoyancy forces drive lithospheric and asthenospheric convection in the continental lithosphere soon after the onset of extension in the continental lithosphere.

In this paper we investigate melt production predicted by a pure–shear model and a UDF model of continental lithosphere thinning leading to seafloor spreading initiation and compare the results to published observations at the Iberian margin. The two models are considered kinematic end-members of the continental breakup lithosphere deformation process; it is probable that the process by which the lithosphere actually deforms is a combination of both. We aim to examine the large scale thermal evolution and consequent first order melt generation predicted by these two models of lithosphere thinning. The continental lithosphere is represented as a continuous homogeneous medium and we do not attempt to model surface features such as faulting.

Seismic surveys across the Iberian margin show a transition zone up to 170 km wide [10,12] between thinned continental and oceanic crust, exposing serpentinised peridotite at the seafloor. Fig. 1 shows an

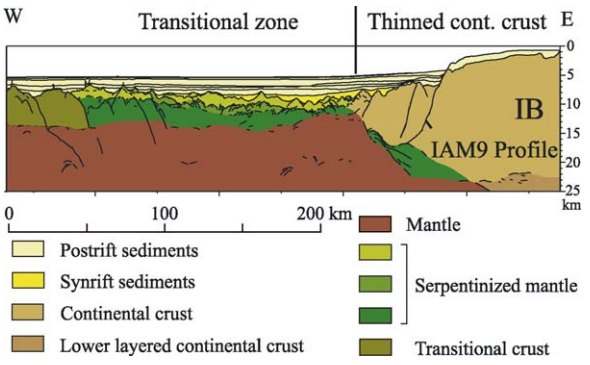

Fig. 1. Line drawing and interpretation along the IAM-9 seismic section across the Iberian margin. Along this section the transition zone between continental and oceanic crust is around 170 km wide. Adapted from [39].

Fig. 1. Dessin au trait et interprétation le long de la coupe sismique IAM-9 à travers la marge ibérique. Le long de cette section, la zone de transition entre croûte occidentale et croûte océanique a environ 170 km de large. Modifié d'après [39].

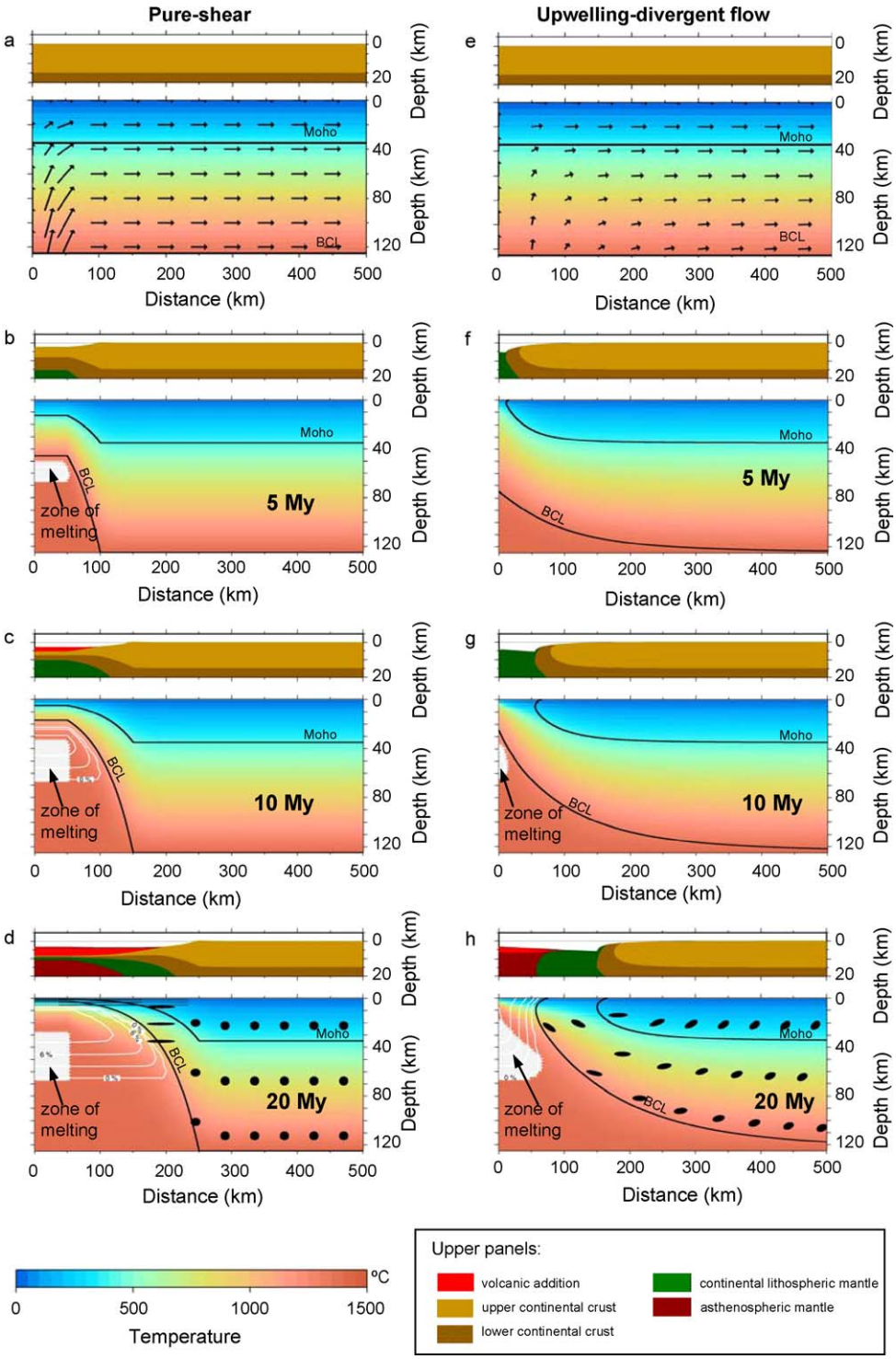

Fig. 2. **a–d** Model evolution of continental lithosphere thinning and seafloor spreading initiation due to a finite width ($W_{1/2} = 50$ km) pure-shear flow-field extending at a half-rate (V_x^0) of 10 mm/yr. Four snapshots in time at **a** $t = 0$, with velocity vectors showing deformation field which is non time-dependent; **b** $t = 5$ Ma, shortly after melt initiation; **c** $t = 10$ Ma and; **d** $t = 20$ Ma. **e –h** Model evolution of continental lithosphere thinning and seafloor spreading initiation due to an upwelling-divergent flow-field with $V_x^0 = V_z^0 = 10$ mm/yr. Four snapshots in time at **e** $t = 0$, with velocity vectors showing deformation field which is non time-dependent; **f** $t = 5$ Ma; **g** $t = 10$ Ma, shortly after melt initiation and; **h** $t = 20$ Ma. In each case the lower panel shows a Eulerian plot of temperature, the zone of melting (grey), depletion (white contours with interval of 3%) and the position of

interpreted line drawing of the IAM-9 seismic refraction profile, where the transition zone is at its widest. Magnetic anomalies in the transition zone are weak and may originate from the emplacement of minor magmatic intrusions [42] or by the serpentinisation of peridotite [39] during progressive exhumation. Petrologic work suggests that the exhumed mantle is subcontinental in origin, and has a complex history of enrichment and depletion [7,27]. Exhumed mantle is present on the Iberian margin and its conjugate, the Newfoundland margin, for around 300 km along strike, varying in width from 50 to 170 km [39]. The seismic velocity structure in the transition zone differs from the structure in adjacent oceanic and thinned continental crust and Moho reflections are weak or absent, indicating the presence of exhumed mantle with decreasing mantle serpentenisation with depth [44]. The seismic velocity structure and the low amplitude of magnetic anomalies in the basement suggest that either no volcanic addition or only minor volcanic addition (probably present as gabbroic intrusions rather than as surface volcanic addition) is present within the ZECM [45,26].

A series of ocean drilling project (ODP) wells, drilled along a profile 40 km north of the IAM-9 profile provide constraints on the timing of margin formation. Shallow water Tithonian (149 Ma) sediments recovered from the tops of continental fault blocks [44] are thought to be pre-rift sediments deposited in a platform environment of a few hundred meters water depth. Isostatic considerations suggest that the crust was around 28–30 km thick at this time [30], although reconstruction of seismic sections implies that the crust may have been only 10 km thick [22]. Plagioclase in gabbros from the lowermost crust exposed at the seafloor on a detachment fault at the landward edge of the transition zone has an Ar–Ar age (indicating the rock cooling below c. 150 °C) of 136.4 ± 0.3 Ma [14]. This implies that significant thinning of the continental crust had occurred by this time. Within the ZECM, depleted subcontinental mantle has been cored without encountering any mafic rocks with a syn-rift intrusion age [45]. Along the IAM-9 profile, magnetic anomaly analysis [42,12,37,39] demonstrates the progressive exhumation of mantle oceanwards, which may have begun as early as the early Berriasian, around 142 Ma [39]. The exhumation of mantle requires that the continental crust is significantly thinned, and probably present only as small discrete allochthons between exposures of exhumed continental mantle. Subsequent exhumation of more than 100 km of continental mantle widened the ZECM at a half-spreading rate of between 6 and 13 mm/yr [39]. Tucholke et al [40] suggest that the rising asthenosphere breached the continental lithosphere at Latest Aptian -Earliest Albian times (112 Ma) and normal seafloor spreading ensued. However the onset of localised seafloor spreading in the area is complex and the exact timing remains uncertain [16,40,31].

Considering the lithological and age constraints from the ODP wells to the north of the section and following [12,26], we have placed the following quantitative limits on the kinematics and characteristics of the Iberian margin along IAM-9:

(1) the continental crust was significantly thinned, so that continental mantle could be exhumed, in less than 15 Ma (from the Tithonian until exhumation of the lowermost crust);
(2) crustal stretching factors (β_{crust}) of more than 10 are required for mantle exhumation to occur (i.e. continental crust less than 3 km thick if the initial crustal thickness was 30 km);
(3) the half-extension (or half-spreading) rate during the formation of the ZECM was 10 mm/yr;
(4) volcanic addition in the transition zone is less than 2 km thick [26];
(5) extension across the Iberian margin, prior to the formation of oceanic crust (i.e. continental extension plus the width of the ZECM), is 150–200 km.

the Moho and base of the continental lithosphere (BCL); the upper panel shows the upper 20 km of the model, bathymetry is calculated from the isostatic response to thermal, crustal thinning, volcanic addition and water loads. Black ellipses in **d** and **h** indicate finite strain since $t = 0$.

Fig. 2. **a** –**d** Évolution du modèle d'initiation de l'amincissement lithosphérique et de l'expansion du plancher océanique, due à un champ d'écoulement de cisaillement pur, de largeur finie ($W_{1/2} = 50$ km), se développant à une demi-vitesse (V_x^0) de 10 mm/an. Quatre repères de fracturation dans le temps à, **a** $t = 0$ avec vecteurs de vitesse montrant le champ de déformation non dépendant du temps ; **b** $t = 5$ Ma, peu de temps après l'initiation de la fusion ; **c** $t = 10$ Ma et **d** $t = 20$ Ma. **e** –**h** évolution de modèle d'initiation de l'amincissement de la lithosphère continentale et de l'expansion du plancher océanique due à un champ « *upwelling* - flux divergent », avec $V_x^0 = V_z^0 = 10$ mm par an. Les 4 repères de fracturation dans le temps à, **e** $t = 0$, avec des vecteurs de vitesse montrant le champ de déformation qui est non dépendant du temps ; **f** $t = 5$ Ma ; **g** $t = 10$ Ma, peu de temps après l'initiation de la fusion, et **h** $t = 20$ Ma. Dans tous les cas, le panneau du bas montre un relevé eulérien de température, la zone de fusion (grise) , de déplétion (contours blancs), la position du Moho et la base de la lithosphère continentale (BCL) ; le panneau supérieur montre les 20 km supérieurs du modèle ; la bathymétrie est calculée à partir de la réponse isostatique à la température, à l'amincissement crustal, aux ajouts volcaniques et à la charge des eaux. Les ellipses noires en **d** et **h** indiquent la contrainte finie puisque $t = 0$.

We model continental breakup using pure–shear and UDF models with half-spreading rates of 10 mm/yr and compare predictions made by the models to observations on the Iberian margin. The effects of a slower extension rate on the predictions of volcanic thickness made by the model are investigated, as there are uncertainties related to the timing of margin formation. The influence of a variable continental geotherm and melt extraction efficiency on model predictions are also presented.

2. Lithosphere thinning by pure–shear

Pure–shear thinning of the lithosphere can be defined as a 1–D velocity field $V_z(z)$, where $V_z(z)$ is the vertical (upwards) velocity and z is depth [17]. To extend this definition into 2–D, we define a deformation field where pure–shear occurs within a fixed half-width, $W_{1/2}$, axial zone in the lithosphere. A wide zone of pure–shear leads to slow thinning of the lithosphere, whereas a narrow zone of pure–shear results in very fast thinning. We assume rifting is symmetrical. In the axial upwelling region the pure–shear deformation velocity field is:

$$V_x(x,z) = V_x^0 \frac{x}{W_{1/2}} \tag{1}$$

$$V_z(x,z) = -V_x^0 \frac{z}{W_{1/2}} \tag{2}$$

Outside of the upwelling region material is simply translated so that:

$$V_x(x,z) = V_x^0 \tag{3}$$

$$V_z(x,z) = 0 \tag{4}$$

$V_x(x,z)$ and $V_z(x,z)$ are the horizontal and upwelling velocities respectively at x and z, the horizontal and vertical coordinates respectively. V_x^0 is the half-extension rate. $V_x(x,z)$ and $V_z(x,z)$ are symmetric about $x = 0$. Half-extension (i.e. extension on one margin), E, is a product of V_x^0 and the duration of rifting t, such that $E = V_x^0 t$. The stretching factor, β, is the ratio between initial and current thickness of a layer such as the crust [24], and the thinning factor, $\gamma = 1 - 1/\beta$. The initial temperature structure of the continental lithosphere is assumed to be in thermal equilibrium so that the initial temperature is:

$$T(x,z)_{(t=0)} = T_0 \frac{z}{a} \tag{5}$$

where T_0 is the mantle potential temperature (1333 °C) and a the lithosphere thickness (assumed to be 125 km). Radiogenic heat productivity is ignored. We model the thermal evolution of the lithosphere using the advection–diffusion equation:

$$\frac{\partial T}{\partial t} = \kappa \nabla^2 T - \mathbf{V} \cdot (\nabla T + h) \tag{6}$$

using the finite difference method, where T is temperature, κ is the thermal diffusivity of the mantle (0.8×10^6 m^2/s^{-1}), $\mathbf{V}$ is the velocity vector and h is the adiabatic gradient (assumed to be 0.3 °C/km). The temperature structure evolves in response to the imposed pure–shear flow-field, reflecting a balance between heat advection and conduction.

The temperature field is used to calculate melt production. If conditions in the model space exceed the solidus of dry peridotite, melting is predicted. We calculate the melt fraction, f, at each node in the model grid as a function of temperature and pressure at each time step using the parameterisation of [18]. The rate of melt production at time t (R_t) depends on the incremental increase in f so that:

$$R_t = \frac{\rho_m}{\rho_v} \int_{-\infty}^{0} \int_{0}^{+\infty} \frac{\partial f}{\partial t} \, \mathrm{d}x \, \mathrm{d}z \text{ when } \frac{\partial f}{\partial t} > 0 \tag{7}$$

Volcanic addition is assumed to have a lower density than the mantle source: ρ_m (3330 kg/m^3) and ρ_v (2850 kg/m^3) are the mantle and volcanic addition densities, respectively. A parcel of mantle material becomes more depleted as it advects though the melting region. Depletion, d, is the maximum f experienced by a parcel of mantle. If melt migration is assumed to be instantaneous and perfectly efficient, the thickness of the layer of volcanic addition can be calculated. For the pure–shear model, melt is assumed to migrate to the surface and is evenly distributed across the upwelling half-width ($W_{1/2}$), subsequently migrating laterally at $\mathbf{V}(x,0)$; the thickness of melt in the axial region at time t (H_t) can be calculated:

$$H_t = \frac{1}{\beta W_{1/2}} \int_0^t R_{t'} \beta_{t'} \, \mathrm{d}t' \tag{8}$$

following [5], where t' is a dummy time variable.

Continental lithosphere material is advected according to the deformation field, and the distribution of depletion is tracked through time. Subsidence or uplift caused by density changes due to thermal effects, crustal thinning or thickening and volcanic addition are calculated assuming local isostasy and water-loading. Fig. 2(a)–(d) shows the temporal evolution of continental breakup by pure–shear, where $V_x^0 = 10$ mm/yr and $W_{1/2} = 50$ km. These parameters result in a stretching factor (β) close to 50 after 20 Myr, corresponding to the critical β used to define breakup by [26] in their application of the pure–shear melting

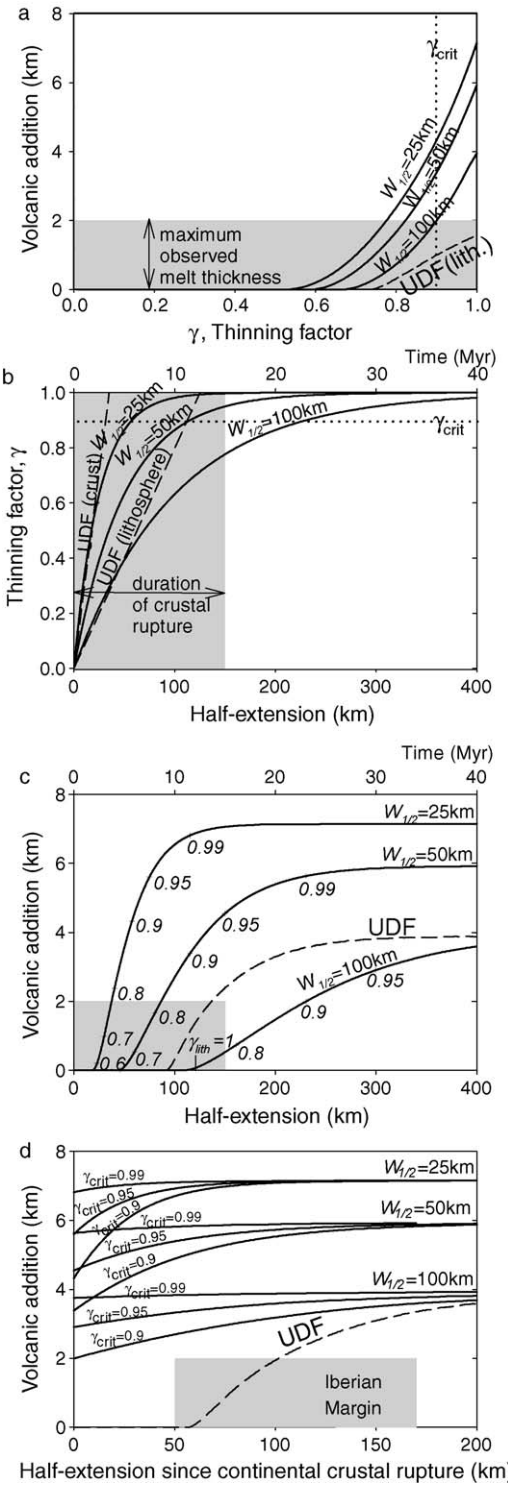

Fig. 3. **a**–**c** Cross-plots of volcanic addition, thinning factor and half-extension (i.e. extension on one margin) predicted by the 2–D pure-shear model run at 10 mm/yr and upwelling half-widths of 25 km, 50 km and 100 km (solid lines) and the upwelling-divergent flow model (dashed lines). Note depth-dependent stretching in the UDF model means that $\gamma_{lith} \neq \gamma_{crust}$. In both cases all parameters are the same except the deformation field. Estimates of observed melt thickness (< 2 km) and duration of complete crustal rupture (< 15 Ma) for the Iberian margin are plotted in grey. γ_{crit} is the assumed critical thinning factor after which mantle exhumation can occur. In **c** '$\gamma_{lith} = 1$' refers to UDF model. **d** Volcanic addition plotted against half-extension since continental crustal rupture (γ_{crit} for the pure-shear model, $\gamma_{crust} = 1$ for the UDF model). The grey box indicates width of ZECM on the Iberian margin. Pure-shear model results are solid lines and the UDF model results are dashed lines. The UDF model predicts exhumation of mantle prior to melt production.

model [5] to the Iberian margin. In the example shown on Fig. 2(a)–(d), melting initiates at 4.6 Ma, after 46 km of half-extension, when the stretching factor in the axial region (where $0 < x < W_{1/2}$) is 2.5. The thickness of volcanic addition increases as the lithosphere continues to thin: when the stretching factor reaches 10, a 3.4 km thick layer of volcanic addition is predicted in the axial region, and after 20 Ma (when the axial stretching factor is 50) the thickness of the volcanic addition is 5.4 km. Crust or lithosphere undergoing pure–shear requires infinite extension to reach zero thickness, but rupture of continental crust (a prerequisite for mantle exhumation) may be considered to occur at a critical crustal thinning factor γ_{crit}, which we assume equals 0.9 ($\beta = 10$).

Cross-plots of melt thickness, thinning factor and half-extension predicted by the pure–shear model with axial half-widths of 25, 50 and 100 km are shown on Fig. 3. More volcanic crust is predicted by the pure–shear model at crustal rupture ($\gamma = 0.9$) than is observed at the Iberian margin (¡2 km thickness), unless the upwelling zone $W_{1/2}$ is wider than 100 km (Fig. 3a). However, if the upwelling zone is very wide, the pure–shear model predicts thinning rates that are too slow to rupture the continental crust within the time available (15 Ma) on the

Fig. 3. **a** –**c** Plots croisés des ajouts volcaniques, du facteur d'amincissement et de la demi-extension (c'est-à-dire de l'extension sur une seule marge) prédits par le modèle de cisaillement pur, développé à 10 mm/an et demi-largeurs d'expansion de 25 km, 50 km et 100 km (lignes continues) et modèle d'« *upwelling*-flux divergent » (lignes tiretées). À noter que l'étirement dépendant de la profondeur dans le modèle UDF signifie que $\gamma_{lith} \neq \gamma_{crust}$. Dans les deux cas, tous les paramètres sont les mêmes, excepté le champ de déformation. Les estimations de l'épaisseur des produits de fusion (< 2 km) et la durée nécessaire à l'obtention de la rupture complète de la croûte (< 15 Ma) pour la marge ibérique sont figurées en gris. γ_{crit} est le facteur d'amincissement critique présumé, selon lequel l'exhumation du manteau prend place. En **c**, « $\gamma_{lith} = 1$ » se réfère au modèle UDF. **d** ajouts volcaniques figurés en regard de la demi-extension, depuis la rupture de la croûte continentale (γ_{crit} pour le modèle de cisaillement pur, $\gamma_{crust} = 1$ pour le modèle UDF). Le compartiment gris indique la largeur ZECM sur la marge ibérique. Les résultats du modèle de cisaillement pur sont figurés par des lignes continues, ceux du modèle UDF par des lignes tiretées. Le modèle UDF prédit l'exhumation du manteau, avant la production de matériel fondu.

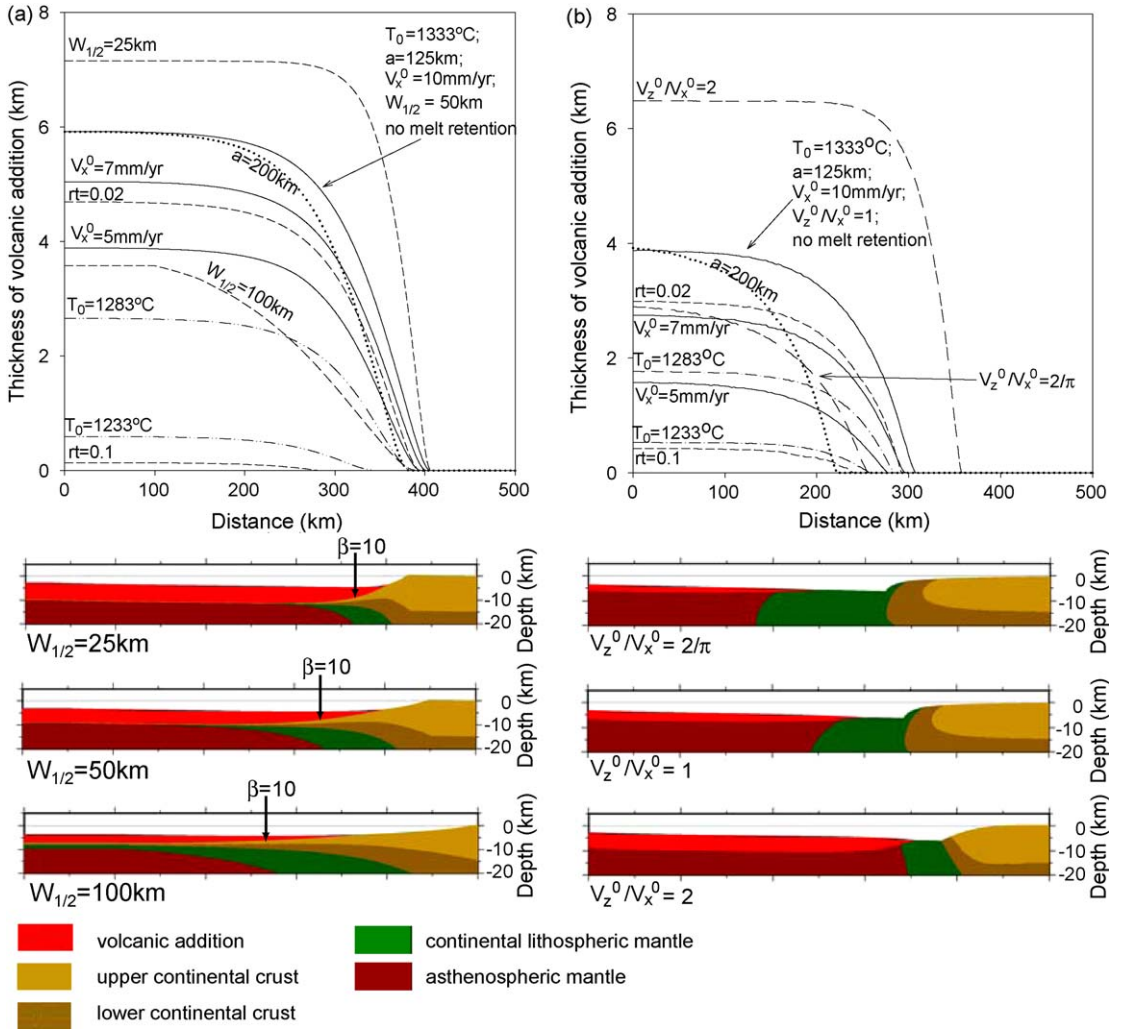

Fig. 4. Thickness of volcanic addition versus horizontal distance plotted for various model parameters for (**a**) pure-shear and (**b**) upwelling-divergent flow models. In (**a**), the median pure-shear model assumes a half-extension velocity of 10 mm/yr, initial lithospheric thickness (*a*) of 125 km, a mantle potential temperature (T_o) of 1333 °C, an upwelling half-width ($W_{1/2}$) of 50 km and perfectly efficient melt extraction. The other curves show results for models run with variable parameters as indicated, otherwise all model parameters are the same as in the median model. The upwelling half-width is the only variable which affects the upper structure and margin geometry (lower panels) predicted by the pure-shear model, the other variables affect only the predicted melt thickness. In (**b**) the median UDF model assumes a half-extension velocity of 10 mm/yr, initial lithospheric thickness (*a*) of 125 km, a mantle potential temperature (T_o) of 1333 °C, a velocity ratio of 1 and perfectly efficient melt extraction. The other curves show results for models run with variable parameters as indicated, otherwise all parameters are the same as in the median model. The velocity ratio is the only variable which affects the upper structure and margin geometry (lower panels) predicted by the UDF model, the other variables affect only the predicted melt thickness. For both sets of results *rt* indicates the degree of melt retention. The first fraction (*rt*) of melt is assumed to remain in the matrix and volcanic addition occurs only after *f* exceeds *rt*. *rt* may also be considered a proxy for the degree of depletion of the continental mantle.

Fig. 4. Épaisseur des produits volcaniques en fonction de la distance horizontale pour différents paramètres du modèle, pour les modèles de cisaillement pur (**a**) et d'« *upwelling*-flux divergent » (**b**). En (**a**), le modèle médian de cisaillement pur suppose une demi-vitesse d'extension de 10 mm/an, une épaisseur lithosphérique (*a*) de 125 km, une température potentielle du manteau (T_o) de 1333 °C, une demi-largeur d'*upwelling* ($W_{1/2}$) de 50 km et une extraction de produits fondus parfaitement efficiente. Les autres courbes montrent des résultats pour des modèles conduits avec des paramètres variables, tels qu'indiqués ; par ailleurs, tous les paramètres sont les mêmes que dans le modèle médian. La demi-largeur d'*upwelling* est la seule variable qui affecte la structure supérieure et la géométrie de la marge (panneaux inférieurs) prédites par le modèle de cisaillement pur ; les autres variables affectent seulement l'épaisseur des produits de fusion prédite. En (**b**), le modèle UDF médian, suppose une demi-vitesse d'extension de 10 mm/an, une épaisseur initiale de la lithosphère (*a*) de 125 km, une température potentielle du manteau (T_o) de 1333 °C, un rapport de vitesse de 1 et une extraction de produits de fusion parfaitement efficiente. Les autres courbes montrent les résultats de modèles fonctionnant avec des paramètres variables, comme indiqués ; par ailleurs, tous les paramètres sont les mêmes que dans le volume médian. Le rapport de vitesse est la seule variable qui affecte le structure supérieure et la géométrie de la marge (panneaux du bas), prédites par le modèle

Iberian margin (Fig. 3(b)). With a mantle potential temperature of 1333 °C, it is not possible to rupture the crust by pure–shear ($\gamma > 0.9$) in less than 15 Ma without producing more than 2 km of volcanic addition (Fig. 3(c)).

Fig. 4(a) illustrates the effects of varying the half-spreading rate, the mantle potential temperature, lithosphere thickness, melt migration efficiency and the upwelling half-width on the thickness of melt predicted by the pure–shear model.

Decreasing the half-extension velocity by a factor of 2 to 5 mm/yr (equivalent to increasing the duration of continental thinning by a factor of 2) causes the onset of melting to occur later due to the effects of conductive cooling. For a model run with the same parameters as that shown on Fig. 2(a)–(d), but at a half-extension rate of 5 mm/yr, melting initiates after 55 km of half-extension (when $\beta = 3$). When the stretching factor reaches 10 (after 23 Ma), a 1.9 km thick layer of volcanic addition is predicted in the axial zone. The thickness of volcanic addition increases to more than 2 km just 1 Ma later, and so based on our criteria may predict up to 5 km width of exhumed mantle, far less than that observed on the Iberian margin. Substantially lower half-extension rates are required to generate the observed width of exhumed mantle, which would require a much longer duration and earlier onset of continental lithosphere thinning.

Decreasing the mantle potential temperature by 100 ° C delays the onset of melting until a thinning factor of 0.88 has been reached, and the thickness of volcanic addition remains below 2 km for the duration of the model. Similarly, if melt migration is inefficient or does not migrate to the surface, or if the asthenospheric mantle (it is predominantly the asthenospheric mantle which partially melts) is highly depleted, the onset of melting is delayed and the thickness of volcanic addition is severely reduced. These results support previous conclusions that the formation of a wide ZECM on the Iberian margin may only be explained by pure–shear lithospheric thinning in the presence of a cool asthenosphere or a much depleted mantle during breakup [26,35,30].

3. Lithosphere thinning by upwelling–divergent flow

We use a cornerflow solution [2] to describe the UDF deformation field during continental break up. The solution and its derivatives have previously been used to describe mid ocean ridge processes [34,6]. The velocity field is defined by a half-spreading rate at the surface, V_x^0, and an axial upwelling rate, V_z^0:

$$V_x(x,z) = -B - D\tan^{-1}\left(\frac{z}{x}\right) + (Cx + Dz)\left(\frac{-x}{x^2+z^2}\right) \tag{9}$$

$$V_z(x,z) = A + C\tan^{-1}\left(\frac{z}{x}\right) + (Cx + Dz)\left(\frac{-z}{x^2+z^2}\right) \tag{10}$$

where:

$$A = 0,\ B = \frac{2\pi V_z^0 - \pi^2 V_x^0}{(\pi^2-4)},\ C = \frac{4V_x^0 - 2\pi V_z^0}{(\pi^2-4)},$$
$$D = \frac{2\pi V_x^0 - 4V_z^0}{(\pi^2-4)}$$

In order to calibrate the model against mid-ocean ridge crustal thickness data, we calculated steady state volcanic addition (oceanic crustal thickness) for a range of velocities, V_z^0/V_x^0 ratios and mantle potential temperatures (Fig. 5). For $V_z^0/V_x^0 = 1$ and $T_0 = 1333$ °C, steady state volcanic addition is predicted to be 5–7 km when the half-spreading rate is above 20 mm/yr. At half-spreading rates less than 20 mm/yr, a higher V_z^0/V_x^0 ratio or higher mantle potential temperature fits the oceanic crustal data better. The UDF model presented here is concerned with the transient period of continental break up prior to steady state seafloor spreading, the dynamics of which are poorly understood. For passive isoviscous divergent flow, $V_z^0/V_x^0 = 2/\pi$ [32]; although a higher V_z^0/V_x^0 ratio is probably a more suitable approximation when temperature and stress-dependent viscosity are considered [38]. For this reason, we assume that $V_z^0/V_x^0 = 1$ during rifted margin formation.

The temperature structure, melt generation and subsidence are calculated in the same way as described for the pure–shear model. All melt is assumed to migrate to the surface at the divergence axis so that:

$$Hc_t = \frac{R_t}{V_x^0} \tag{11}$$

where Hc_t is the thickness of the volcanic layer produced at the axis at time t. The surface volcanic layer subsequently moves laterally away from the axis at V_x^0.

UDF ; les autres variables affectent seulement l'épaisseur des produits de fusion prédite. Pour les deux séries de résultats, *rt* indique le degré de rétention des produits de fusion. La première fraction de *rt* est supposée rester dans la matrice et l'ajout volcanique se produit seulement après que *f* dépasse *rt*; *rt* peut aussi être considéré comme un proxy pour le degré de déplétion du manteau continental.

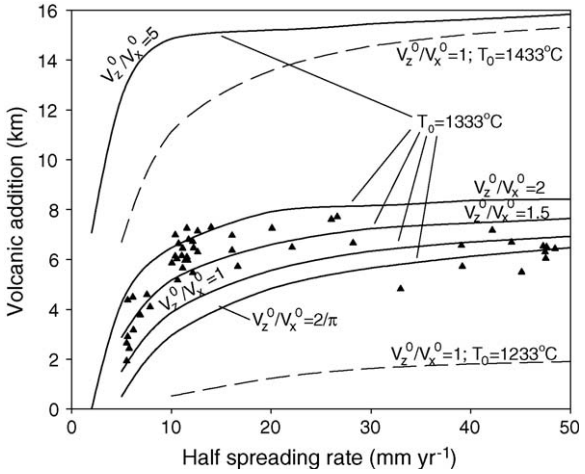

Fig. 5. Crustal thickness predicted by the UDF model at steady state, showing the sensitivity of the model to mantle potential temperature and V_z^0/V_x^0ratio. Unless stated, the steady state crustal thickness is calculated with $V_z^0/V_x^0 = 1$ and $T_0 = 1333\,^{\circ}\mathrm{C}$. Solid triangles indicate seismically defined oceanic crustal thicknesses at mid-ocean ridges (Data-points from ref. [41]).

Fig. 5 Épaisseur crustale prédite par le modèle UDF à l'état stable, montrant la sensibilité du modèle à la température potentielle du manteau et au rapport V_z^0/V_x^0. Á moins qu'elle ne soit établie, l'épaisseur de la croûte à l'état stable est calculée avec $V_z^0/V_x^0 = 1$ et $T_0 = 1333\,^{\circ}\mathrm{C}$. Les triangles pleins indiquent les épaisseurs de la croûte océanique sismiquement définies dans les rides médio-atlantiques (données d'après réf. [41]).

Fig. 2(e)–(h) shows the temporal evolution of a model of continental break-up due to UDF with $V_x^0 = V_z^0 = 10$ mm/yr. As the model evolves, the flow-field causes the thinning and rupture of the upper crust and progressive exhumation of deeper lithosphere layers. At a time of 9.8 Ma, after a 98 km-wide section of continental crust and mantle has been exhumed, the first melt is produced as the temperature–pressure conditions in the model cross the dry peridotite solidus at a depth of around 55 km under the axis. As the model thermally evolves, the zone of melting becomes wider and the thickness of volcanic addition increases, until approximately 30 Ma, when the amount of melt produced reaches a steady state (Fig. 3(c)). Assuming an initial crustal thickness of 35 km, the UDF model predicts rupture of the continental crust after just 35 km of half-extension, before rupture of the continental lithosphere (Fig. 3(b)). The UDF model predicts that mantle exhumation begins after much less upper lithosphere extension than the pure–shear models. Predicted volcanic addition as a function of lithosphere thinning is also much less for the UDF model than the pure–shear model (Fig. 3(a)). The UDF model predicts that melt generation commences after 98 km of horizontal lithosphere half-extension (Fig. 3(c)), several Ma after rupture of the continental crust, and (assuming an initial crustal thickness of 35 km) 63 km of continental mantle is exhumed prior to the initiation of melting (Fig. 3(d)). At a lithosphere thinning factor of 1 (after 125 km of half-extension) the UDF models predicts approximately 1 km of volcanic addition, which is within the range observed for the Iberian margin. Fig. 4(b) illustrates the effects of varying the mantle potential temperature, lithosphere thickness, half-spreading rate, melt migration efficiency and the velocity ratio (V_z^0/V_x^0) on the thickness of melt predicted by the UDF model. The amount of extension prior to the onset of melting, and consequentially the width of the ZECM predicted by the UDF model is more sensitive to the above factors than the pure–shear model. A wide zone of exhumed mantle is favoured when continental lithosphere thinning and rupture occurs with a low mantle potential temperature, initially thick continental lithosphere, slow extension rates, poor melt migration efficiency or high levels of depletion or with a low velocity ratio.

The mode of deformation which occurs during rifted margin formation is a complex function of the initial temperature and compositional structure of the (heterogeneous) lithosphere and the extension rate [13,1,15]. For the UDF model, a higher velocity ratio flow predicts a narrower margin structure and a narrower zone of exhumed mantle than if the velocity ratio is low (Fig. 4(b)), and may be more appropriate for volcanic margins [21]. High velocity ratio flow may be more likely to occur if the lower lithosphere is initially, weak, hot or pre thinned [29].

4. Discussion

A ZECM, up to 170 km wide, between the continental and oceanic crust, is observed at the Iberian continental margin. No syn-breakup volcanic addition has been directly observed in the ZECM, and seismic data indicate that a thickness of less than 2 km of magmatic origin is present. We show that the pure–shear model of continental thinning predicts more than 2 km of volcanic addition when the continental crustal ruptures ($\beta > 10$) in less than 15 Ma. There are a number of possible explanations for the paucity of extrusive or shallow intrusive volcanism. If continental lithosphere thinning by pure–shear occurred over a much longer period of time, conductive cooling may suppress the onset of melting. However, the thinning and extension rates required to explain the formation of a wide (many tens of kilometres or more) zone of exhumed mantle are much

slower than those thought to have been active during the formation of the Iberian margin and would require a much earlier onset in order to rupture the continental crust by 136 Ma. It is possible that melting during formation of the Iberian margin was inhibited due to low mantle potential temperatures (100 ° C lower) [26,35] or the presence of depleted ($>10\%$ depletion) [30] asthenospheric mantle beneath the Iberian–Newfoundland rift during the breakup process. Another possible explanation is that, early in the breakup process, melt migration to the surface was hindered by freezing or impermeability some distance ahead of the solidus (recorded as the first depletion contour). On the Tethyan non-volcanic rifted margin in the Alps and on the Galician margin (100 km north of IAM-9), exhumed mantle shows evidence of syn-break-up infiltration by asthenospheric melt [28,7], showing that complete melt extraction does not always occur in the early stages of rifting and seafloor spreading at non-volcanic rifted margins. It is possible that some melt is distributed throughout the lithosphere under the transition zone, although it is unlikely to be able to account for a very wide zone of exhumed mantle as melt quickly forms migration pathways at low melt fractions [25].

Another possibility, which we have focused on, is that pure–shear is not the dominant mechanism of continental lithosphere thinning leading to breakup and seafloor spreading initiation. Fig. 3(d) shows volcanic addition as a function of half-extension since crustal rupture ($\gamma = \gamma_{crit}$ for the pure–shear model and where crustal thickness is 0 [$\gamma_{crust} = 1$] for the UDF model) predicted by the two models for a half-spreading rate thought to be applicable to the Iberian margin (10 mm/yr). For both pure–shear and UDF models, melting is delayed in the transient stages of continental breakup due to the upwelling of initially cool lithospheric material and slow spreading rates. Continental lithosphere breakup due to UDF predicts the exhumation of more than 50 km of continental mantle prior to the initiation of melting. The UDF model predicts mantle exhumation because it thins the continental crust more rapidly than the lithosphere and as a consequence the crust ruptures before melt generation begins. In contrast, the pure–shear model thins the crust and lithosphere at the same rate. The ability of the UDF model to predict a wide ZECM prior to the onset of melting and volcanic addition suggests that UDF may play a role in the formation of non-volcanic rifted margins. The pure–shear and UDF models of lithosphere thinning are intended to represent end-member models, however, it is probable that UDF operates together with pure–shear deformation. A pure–shear contribution to lithosphere thinning is clearly indicated by faulting in the upper brittle layer (10 km) of the continental crust prior to breakup.

The UDF model presented here predicts a 63 km-wide zone of exhumed continental mantle whereas the ZECM of the Iberian margin is up to 170 km wide. So whilst the UDF model can partially explain the exhumation of mantle prior to melt initiation at non-volcanic rifted margins, compositional and temperature heterogeneities in the mantle may also play an important role in retarding the onset of melting during breakup, and could also be responsible for lateral variability of volcanism observed at rifted margins.

To further assess the possible contribution of UDF deformation to lithosphere thinning leading to continental breakup, other predictions made by the models can be examined. The overall margin structure predicted by the UDF model differs from that predicted by the pure–shear model. The UDF model predicts progressive exhumation of wide zones of the lower continental crust and mantle, whilst the pure–shear model predicts that much narrower zones of lower continental crust and mantle would be exhumed, even if melting did not occur. On the Iberian margin, lower crustal material was found at the seafloor on the landward side of the transition zone by drilling [43,44], although the continental crust at the seafloor does not typically exhibit the high seismic velocities expected of the lower crust. The transition zone peridotites from the ocean floor have a heterogeneous but depleted subcontinental origin, an observation which may support the UDF model.

The two models differ in their predictions of strain and rotation, the distribution of depletion (Fig. 2), and the pressure temperature history of the exposed mantle. However, measuring these differences may be difficult due to inherited strain, compositional heterogeneities and overprinting of signals during serpentinisation. Continued sampling of the Iberian and other non-volcanic rifted margins may enable further discrimination between the two models and place constraints on their relative importance.

5. Conclusion

A wide ZECM at the Iberian rifted continental margin is difficult to explain if pure–shear is assumed to be the dominant mechanism of continental lithosphere thinning leading to crustal rupture and breakup. Factors such as a cooler mantle, inherited depleted mantle and inefficient melt migration can explain why extrusive volcanism is not observed within the ZECM. However, it is also possible that other lithosphere deformation

processes play an important role during continental breakup. UDF, the flow-field envisaged at mid-ocean ridges, predicts exhumation of the lower crust and subcontinental mantle during continental break up and seafloor spreading initiation, consistent with observations on the Iberian margin. We therefore propose that UDF may play an important role during non-volcanic rifted margin formation.

Acknowledgements

The authors acknowledge constructive reviews by Garry Karner and two anonymous reviewers for their comments which significantly improved this paper. RJF thanks NERC for a research studentship. We also acknowledge the Margin Modelling Phase 2 (MM2) partners (BP, ConocoPhillips, Statoil Hydro, Shell, Petrobras, TOTAL, BG, BHP–Billiton). The GMT software of P. Wessel and W. H. F. Smith was used to construct several figures.

References

[1] G. Bassi, Factors controlling the style of continental rifting: insights from numerical modeling, Earth Planet. Sci. Lett. 105 (1991) 430–452.

[2] G. Batchelor, An Introduction to Fluid Dynamics, Cambridge University Press, New York, 1967.

[3] G. Boillot, M. Recq, E.L. Winterer, A.W. Meyer, J. Applegate, M. Baltuck, J.A. Bergen, M.C. Comas, T.A. Davies, K. Dunham, C.A. Evans, J. Girardeau, G. Goldberg, J. Haggerty, L.F. Jansa, J.A. Johnson, J. Kasahara, J.P. Loreau, E. Lunasierra, M. Moullade, J. Ogg, M. Sarti, J. Thurow, M. Williamson, Tectonic denudation of the upper mantle along passive margins: a model based on drilling results (ODP leg-103, western Galicia margin, Spain), Tectonophysics 132 (1987) 335–342.

[4] G. Boillot, G. Feraud, M. Recq, J. Girardeau, Undercrusting by serpentinite beneath rifted margins, Nature 341 (1989) 523–525.

[5] J.W. Bown, R.S. White, Effect of finite extension rate on melt generation at rifted continental margins, J. Geophys. Res. Solid Earth 100 (1995) 18011–18029.

[6] M.G. Braun, G. Hirth, E.M. Parmentier, The effects of deep damp melting on mantle flow and melt generation beneath mid ocean ridges, Earth Planet. Sci. Lett. 176 (2000) 339–356.

[7] G. Chazot, S. Charpentier, J. Kornprobst, R. Vannucci, B. Luais, Lithospheric mantle evolution during continental break up: The West Iberia non-volcanic passive margin, J. Petrology 46 (2005) 2527–2568.

[8] P. Chenet, L. Montadert, H. Gairaud, D. Roberts, Extension ratio measurements on the Galicia, Portugal, and northern Biscay continental margins: implications for evolutionary models of passive continental margins, in: Studies in Continental Margin Geology, AAPG Mem. 34, 1982, pp. 703–715.

[9] D.P. Chian, C. Keen, I. Reid, K.E. Louden, Evolution of non-volcanic rifted margins: new results from the conjugate margins of the Labrador sea, Geology 23 (1995) 589–592.

[10] D.P. Chian, K.E. Louden, T.A. Minshull, R.B. Whitmarsh, Deep structure of the ocean-continent transition in the southern Iberia Abyssal Plain from seismic refraction profiles: Ocean drilling program (legs 149 and 173) transect, J. Geophys. Res. Solid Earth 104 (1999) 7443–7462.

[11] M. Davis, N.J. Kusznir, Depth-dependent lithospheric stretching at rifted continental margins, in : G. Karner (Ed.), Proceedings of NSF Rifted Margins Theoretical Institute, Columbia University Press, 2004, pp. 92–136.

[12] S.M. Dean, T.A. Minshull, R.B. Whitmarsh, K.E. Louden, Deep structure of the ocean-continent transition in the southern Iberia Abyssal Plain from seismic refraction profiles: The IAM-9 transect at 40 degrees 20′ N, J. Geophys. Res. Solid Earth 105 (2000) 5859–5885.

[13] J.A. Dunbar, D.S. Sawyer, How preexisting weaknesses control the style of continental breakup, J. Geophys. Res. Solid Earth Planets 94 (1989) 7278–7292.

[14] G. Féraud, M. O. Beslier, G. G. Cornen, ^{40}Ar– ^{39}Ar dating of gabbros from the ocean–continent transition of the western Iberia margin: preliminary results, in: R.B., Whitmarsh, D.S., Sawyer, A., Klaus, D.G., Masson, (Eds.), Proceedings of the Ocean Drilling Program, Scientific Results, vol. 149, Ocean Drilling Program, College Station, Texas, 1996, pp. 489–495.

[15] D.L. Harry, J.C. Bowling, Inhibiting magmatism on nonvolcanic rifted margins, Geology 27 (1999) 895–898.

[16] O. Jagoutz, O. Muntener, G. Manatschal, D. Rubatto, G. Peron-Pinvidic, B.D. Turrin, I.M. Villa, The rift-to-drift transition in the North Atlantic: A stuttering start of the MORB machine? Geology 35 (2007) 1087–1090.

[17] G.T. Jarvis, D.P. McKenzie, Sedimentary basin formation with finite extension rates, Earth Planet. Sci. Lett. 48 (1980) 42–52.

[18] R.F. Katz, M. Spiegelman, C.H. Langmuir, A new parameterization of hydrous mantle melting, Geochem. Geophy. Geosys. 4 (2003) 1073.

[19] N. J. Kusznir, G. D. Karner, Continental lithospheric thinning and breakup in response to upwelling divergent mantle flow: application to the Woodlark, Newfoundland and Iberia margins, in: G.D., Karner, G., Manatschal, L.M., Pinheiro, (Eds.), Imaging, Mapping and Modelling Continental Lithosphere Extension and Breakup, vol. 282 of special publications, Geological Society, London, 2007, pp. 389–419.

[20] N.J. Kusznir, R. Hunsdale, A.M. Roberts, Timing of depth-dependent lithosphere stretching on the S. Lofoten rifted margin offshore mid-Norway: pre-breakup or post-breakup? Basin Research 16 (2004) 279–296.

[21] N. Kusznir, R. Hunsdale, A. M. Roberts, iSIMM Team, Timing and magnitude of depth-dependent lithosphere stretching on the southern Lofoten and northern Vøring continental margins offshore mid-Norway: implications for subsidence and hydrocarbon maturation at volcanic rifted margins, in: A. Dore, B. Vining, (Eds.), Petroleum Geology: Northwest Europe and Global Perspectives: Proceedings of the 6th Petroleum Geology Conference, Geological Society, London, 2005, pp. 757–783.

[22] G. Manatschal, New models for evolution of magma-poor rifted margins based on a review of data and concepts from West Iberia and the Alps, Inter. J. Earth Sci. 93 (2004) 432–466.

[23] G. Manatschal, D. Bernoulli, Architecture and tectonic evolution of nonvolcanic margins: Present-day Galicia and ancient Adria, Tectonics 18 (1999) 1099–1119.

[24] D. McKenzie, Some remarks on the development of sedimentary basins, Earth Planet. Sci. Lett. 40 (1978) 25–32.

[25] D. McKenzie, Some remarks on the movement of small melt fractions in the mantle, Earth Planet. Sci. Lett. 95 (1989) 53–72.
[26] T. A. Minshull, S. M. Dean, R. S. White, R. B. Whitmarsh, Anomalous melt production after continental break up in the southern Iberia Abyssal Plain, in: R.C., Wilson, R.B., Whitmarsh, B., Taylor, N., Frotzheim, (Eds.), Non volcanic Rifting of Continental Margins: A Comparison of Evidence from Land and Sea, vol. 187 of special publications, Geological Society, London, 2001, pp. 537–550.
[27] O. Muntener, G. Manatschal, High degrees of melt extraction recorded by spinel harzburgite of the Newfoundland margin: The role of inheritance and consequences for the evolution of the southern North Atlantic, Earth Planet. Sci. Lett. 252 (2006) 437–452.
[28] O. Muntener, T. Pettke, L. Desmurs, M. Meier, U. Schaltegger, Refertilization of mantle peridotite in embryonic ocean basins: trace element and Nd isotopic evidence and implications for crust–mantle relationships, Earth Planet. Sci. Lett. 221 (2004) 293–308.
[29] T.K. Nielsen, J.R. Hopper, From rift to drift: Mantle melting during continental breakup, Geochem. Geophys. Geosys. 5 (2004) 07003.
[30] M. Pérez-Gussinyé, J.P. Morgan, T.J. Reston, C.R. Ranero, The rift to drift transition at non-volcanic margins: Insights from numerical modelling, Earth Planet. Sci. Lett. 244 (2006) 458–473.
[31] G. Peron-Pinvidic, G. Manatschal, T. A. Minshull, D. S. Sawyer, Tectonosedimentary evolution of the deep Iberia–Newfoundland margins: Evidence for a complex breakup history, Tectonics 26 (2)1.
[32] J. PhippsMorgan, Melt migration beneath mid ocean spreading centers, Geophys. Res. Lett. 14 (1987) 1238–1241.
[33] S.L.B. Pickup, R.B. Whitmarsh, C.M.R. Fowler, T.J. Reston, Insight into the nature of the ocean–continent transition off west Iberia from a deep multichannel seismic reflection profile, Geology 24 (1996) 1079–1082.
[34] I. Reid, H.R. Jackson, Oceanic spreading rate and crustal thickness, Marine Geophys. Res. 5 (1981) 165–172.
[35] T.J. Reston, J.P. Morgan, Continental geotherm and the evolution of rifted margins, Geology 32 (2004) 133–136.
[36] L. Royden, C.E. Keen, Rifting process and thermal evolution of the continental margin of eastern Canada determined from subsidence curves, Earth Planet. Sci. Lett. 51 (1980) 343–361.
[37] S.M. Russell, R.B. Whitmarsh, Magmatism at the West Iberia non-volcanic rifted continental margin: evidence from analyses of magnetic anomalies, Geophys. J. Int. 154 (2003) 706–730.
[38] Y. Shen, D.W. Forsyth, The effects of temperature-dependent and pressure-dependent viscosity on 3-dimensional passive flow of the mantle beneath a ridge-transform system, J. Geophys. Res. Solid Earth 97 (1992) 19717–19728.
[39] J. C. Sibuet, S. Srivastava, G. Manatschal, Exhumed mantle–forming transitional crust in the Newfoundland-Iberia rift and associated magnetic anomalies, J. Geophys. Res. Solid Earth 112 (B6).
[40] B. E. Tucholke, D. S. Sawyer, J. C. Sibuet, Breakup of the Newfoundland Iberia rift, Geological Society, London, Special Publications 282 (2007) 9–46.
[41] R.S. White, T.A. Minshull, M.J. Bickle, C.J. Robinson, Melt generation at very slow-spreading oceanic ridges: Constraints from geochemical and geophysical data, J. Petrology 42 (2001) 1171–1196.
[42] R.B. Whitmarsh, P.R. Miles, Models of the development of the West Iberia rifted continental margin at 40-degrees-30N deduced from surface and deep-tow magnetic-anomalies, J. Geophys. Res. Solid Earth 100 (1995) 3789–3806.
[43] R.B. Whitmarsh, S.M. Dean, T.A. Minshull, M. Tompkins, Tectonic implications of exposure of lower continental crust beneath the Iberia Abyssal Plain, Northeast Atlantic Ocean: Geophysical evidence, Tectonics 19 (2000) 919–942.
[44] R.B. Whitmarsh, G. Manatschal, T.A. Minshull, Evolution of magma-poor continental margins from rifting to seafloor spreading, Nature 413 (2001) 150–154.
[45] R. B. Whitmarsh, T. A. Minshull, S. M. Russell, S. M. Dean, K. E. Louden, D. Chian, The role of synrift magmatism in the rift-to-drift evolution of the West Iberia continental margin: geophysical observations, in: R.C., Wilson, R.B., Whitmarsh, B., Taylor, N., Frotzheim, (Eds.), Non volcanic Rifting of Continental Margins: A Comparison of Evidence from Land and Sea, vol. 187 of special publications, Geological Society, London, 2001, pp. 107–124.